We are IntechOpen, the world's leading publisher of Open Access books Built by scientists, for scientists

4,800
Open access books available

122,000
International authors and editors

135M
Downloads

Our authors are among the

154
Countries delivered to

TOP 1%
most cited scientists

12.2%
Contributors from top 500 universities

WEB OF SCIENCE™

Selection of our books indexed in the Book Citation Index in Web of Science™ Core Collection (BKCI)

Interested in publishing with us?
Contact book.department@intechopen.com

Numbers displayed above are based on latest data collected.
For more information visit www.intechopen.com

2

Data Analysis and Simulations of the Large Data Sets in the Galactic Astronomy

Eduardo B. de Amôres
SIM - Faculdade de Ciências da Universidade de Lisboa
Portugal

1. Introduction

In the last decades large data sets covering a wide range of both resolution and observed regions have been accumulated in the Astronomy. Follow-up technology involving the storage and the access to these data is also necessary to develop methods and tools that will allow their usage.

In this chapter, I will review the use of the large data sets in the galactic astronomy, most of them covering almost entire area of the sky in the several wavelengths, for both the diffuse data provided by IRAS, DIRBE/COBE, molecular and hydrogen surveys and point sources catalogues as provided by stellar large-scale surveys such as DENIS, 2MASS, SDSS, among others. A brief description of these surveys and how to access them in the context of Virtual Observatory will be also presented.

Numerical simulations have an important role in understanding and describing the nature of the observations. Particularly, large-scale surveys data can be also used to validate numerical models. I will present models and methods that describe the Galactic structure taking into account the hydrogen atomic distribution in our Galaxy, obtaining galactic parameters such as scale-height, spiral arms parameters, the co-rotation radius.

One of the biggest problems describing the spiral arms in the Galaxy from the gas distribution resides in the fact that some interpretations in the literature for ℓ-v the diagrams have not been updated in respect to rotation curves using old values for the distance from the Sun to the Galactic center. Another problem resides of the difficulty in describing the non-circular motion.

My choice in the present work is to describe the spiral structure by adopting an empirical model (section 3) which is based on the analysis of HI distribution by means its tangential directions and the observed ℓ-v. One of the aims of the present paper is to carry out self consistent inter-comparisons of our results regarding different tracers of the spiral structure.

The models of the spiral structure presented here were first introduced by Amôres & Lépine (2005, AL05) in which two models were proposed to describe the interstellar extinction in the Galaxy (see section 4 of this chapter). Model S consists in obtaining extinction predictions taking into account the spiral structure of our Galaxy. In this model, the extinction grows by steps each time a spiral arm is crossed and remains almost constant in the inter-arm regions. The models were also compared with other samples of objects and regions as pointed by Amôres & Lépine (2007).

As galactic interstellar extinction is a crucial obstacle when observing in the highly obscured regions, it is important to model it properly. I will present the recent efforts in this area. I

will present my model for interstellar extinction, its applications and comparisons with other models and maps available in the context of the Virtual Observatory called GALExtin. Star counts models are also important if one wants to estimate the counts that will be observed by large surveys (GAIA, DES, VVV, LSST, among others). A few simulations for large surveys using star counts are presented in section 5. Conclusions and final remarks are presented in section 6.

2. Large data sets

Large data sets are very important in whole Astronomy. In combination with models these can be used to construct methods to analyze and to interpretate the observed data. They can also be used in order to tune models allowing obtain the best values for a given set of parameters.

Particularly in the galactic Astronomy they can be used in order to obtain parameters of the galactic components, as the thin and thick disk, bulge, bar and galactic halo. Figure 1 shows a representation of our Galaxy structure that is composed basically of four components: disk (thin and thick), bulge, bar and halo. In the disk there is a presence of the spiral arms with young stars while in the halo there are most of the old stars (Robin et al. 2003 and references therein). The shape and properties for each component can be obtained by adjusting parameters of the galactic halo (such as eccentricity, shape) that can also allow us to identify, for instance, the existence of streams and satellite galaxies. (Majewski et al. 2003).

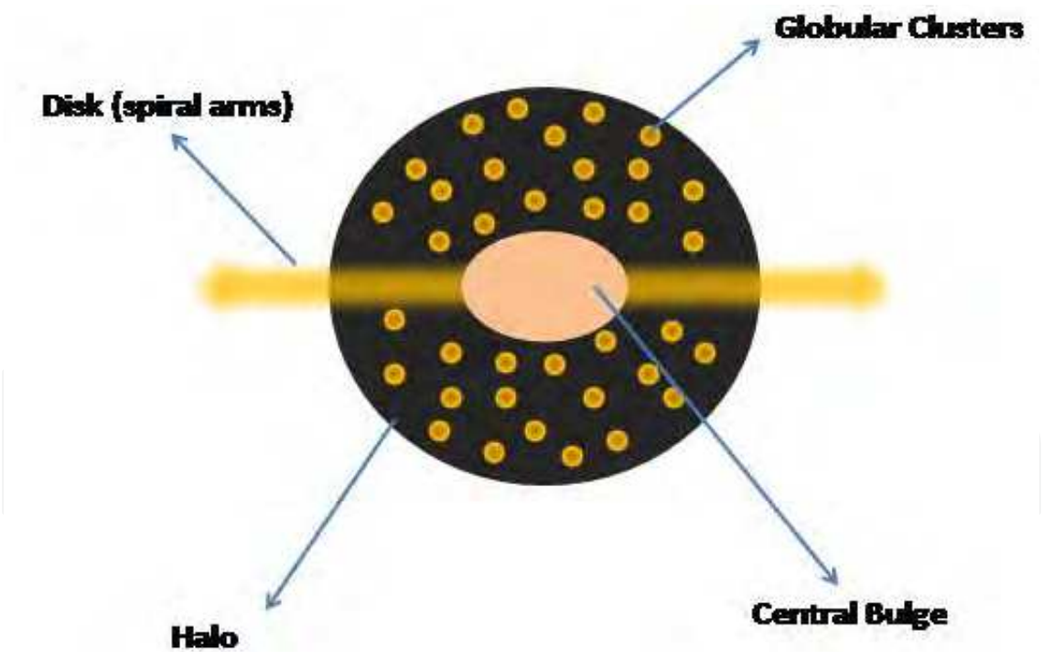

Fig. 1. Schematic Milky Way scheme

On the other hand, large data sets in the galactic Astronomy have an advantage to expand to a wide range of wavelength, from radio to high-energies. The first large surveys were obtained in the radio wavelengths in the decades of 1950-1960 (Kerr 1969) observing atomic hydrogen or HI. The author showed for the first time some interesting aspects of our Galaxy structure, as the warp, flare, spiral arms, among others and be also useful in the

extragalactic astronomy, like for instance the extinction maps elaborated by Burstein & Heiles (1978,1982) based on them. The most recent HI survey is based on the LAB (Leiden-Argentine-Bonn) survey that observed each point of the sky spaced by 0.5 and 0.25 degrees for galactic longitude and latitude producing for each one, what is called spectrum, i.e. the variation of intensity with velocity (Kalberla et al. 2005).

Figure 2 shows the distribution of the integrated intensity, i.e. the sum of the spectra for each coordinate, for all-sky as observed by LAB survey. It can be seen that most of the emission is concentrated for galactic latitudes $|b| \leq 15^o$, denoted by green, yellow and red colors but a significant part of the emission extended up to $|b| \sim 50^o$. One can see a long tail in the emission ranging from 120^o to 200^o reaching south galactic pole.

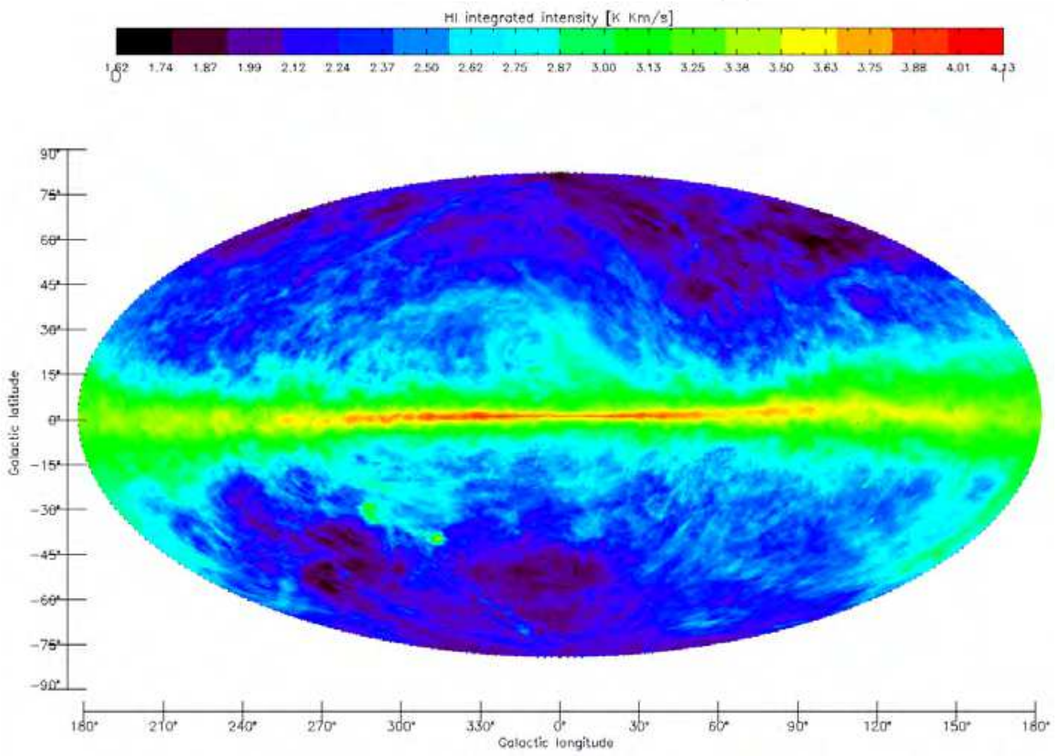

Fig. 2. Map for integrated intensity for neutral hydrogen in galactic coordinates obtained from LAB survey (Kalberla et al. 2005).

Table 1 shows some large surveys useful for galactic structure studies based on other wavelengths as CO that is particularly interesting to identify star-formation regions. Due to the distribution of the interstellar dust in the galactic plane, it obscurates the observations in some wavelengths as in the optical, for instance. Observations performed at infrared wavelengths penetrate through the dust grains and allow us to observe beyond. An extraordinary advance in the study of galactic structure was obtained with IRAS satellite (1983) that observed almost 96% of the sky in four infrared bands followed by DIRBE/COBE experiment in 1992.

Catalogs with stellar sources, as 2MASS (Cutri et al. 2003), SDSS, are also very important in the study of the galactic structure. Concerning 2MASS, Skrutskie et al. (2006) published a catalog which contains 1,647,599 observed extended sources using the classification

algorithms provided by Jarett et al. (2000). As this catalog also contains sources with bad photometry quality, contamination or confusion source due to either intrinsic 2MASS properties or high crowded fields for more detailed works is mandatory to select those sources in respect to quality criteria.
Figure 3 shows a map in galactic coordinates for 2MASS extended sources for all-sky with region observed by Vista Variable in the Via Láctea (VVV) survey (Minniti et al. 2010) region (bulge and disk) represented by white dashed line. The grid of this map is one squared degree for both longitude and latitude.

3. Simulating galactic structure from HI data

This section is organized as follows. Section 3.1 presents the data used in the present work, an analysis from the main emission peaks observed in the HI and CO galactic distribution is presented in section 3.2. Section 3.3 presents the procedure adopted for describing the spiral arms as well the galactic rotation curve used in the present work. The ℓ -v diagrams obtained from the fitting of the parameters of the spiral arms for the HI is presented in section 3.4. A discussion concerning the co-rotation point in our Galaxy is presented in section 3.5.

Wavelength	Survey	Coverage	References
HI	Berkeley	$10^o < \ell < 250^o$ ($\|b\| \leq 10^o$)	Weaver & Williams (1973)
	Parkes	$240^o < \ell < 350^o$ ($\|b\| \leq 10^o$)	Kerr et al. (1986)
	NRAO	$-11^o < \ell < 13^o$	Burton & Liszt (1983)
	LAB	All-Sky	Kalberla et al. (2005)
Near infrared	2MASS (point sources)	All-Sky	Cutri et al. (2003)
	2MASS (extended sources)	All-Sky	Skrutskie et al. (2006)
Optical	SDSS	10,000 square degrees	Adelman-McCarthy et al., (2009)
Proper motion	UCAC-3	All-Sky	Zacharias et al. (2010)
Mid and far-infrared	IRAS	All-Sky	Hauser et al. (1984)
Near/mid and far-infrared	DIRBE/COBE	All-Sky	DIRBE Explanatory Supplement
CO	Dame	$0^o < \ell < 360^o$ ($\|b\| \leq 10^o$)	Dame et al. (1987,2001)
	Stony-Brook	part of galactic plane	Clemens et al. (1986)

Table 1. List of some of the main surveys used in the galactic structure studies.

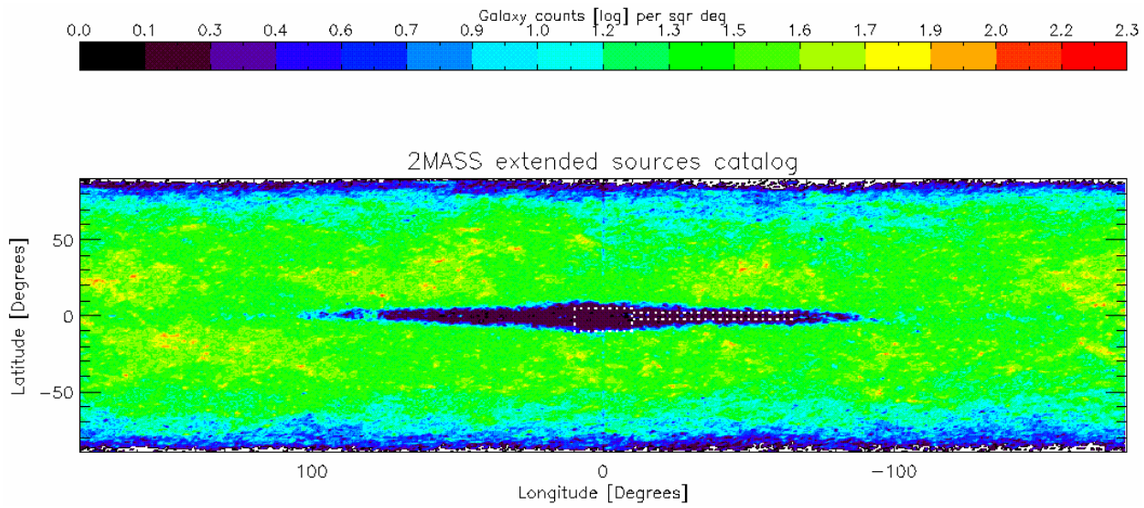

Fig. 3. Galaxy counts obtained by 2MASS. Dashed white line represents regions observed by VVV.

3.1 Data

Hartmann & Burton (1997) published a HI survey based on observations called Leiden/Dwingeloo HI survey that mapped the 21-cm spectral line emission over the entire sky above declinations of -30 degrees using a grid spacing of ~ 0.5 degree and a velocity sampling of ~ 1.03 km/s.

Kalberla et al. (2005) published the LAB (Leiden/Argentine/Bonn) survey which contains the final data release of observations of 21-cm emission from Galactic neutral hydrogen over the entire sky, merging the Leiden/Dwingeloo Survey of the sky north of -30º with the Instituto Argentino de Radioastronomia Survey of the sky south of -25º. The angular resolution of the combined material is HPBW ~ 0.6º. One of the improvements of this new survey consists of also doing corrections on the stray radiation. The LAB survey has been extensibly used in several applications as pointed by Bajaja et al. (2005), Kalberla et al. (2005), Haud & Kalberla (2007), Kalberla & Haud (2006) among others.

In the present chapter, I have employed the HI data from the LAB survey. This data comprises galactic longitudes from 0º to 360º and galactic latitudes from -90º to 90º for both the intervals the 0.5º and up to 1 km/s in velocity. The data are stored in 720 (b,v) fits file maps at longitude intervals stepped by 0.5º.

3.2 The HI and CO main emission complexes

The ℓ-v diagram constitutes an important and useful tool in studying the galactic structure. Reproducing it allows us to obtain relevant information about the distribution, the position and the gas density in the spiral arms, etc. Furthermore, the visualization and interpretation of the ℓ-v diagrams is also essential for their comparison with ones obtained from the predicted models, allowing us to analyze the structures that correspond to the spiral arms from the qualitative point of view, and also to obtain information about the velocity field for the HI and CO.

One way to perform a qualitative study of the ℓ-v diagram consists of estimating the points which correspond to the main peaks for these two gas components from their observed spectra. This task can be performed by fitting the gaussian for the observed HI and CO

spectra. This procedure allows us to identify the regions that delineate the main structures observed in the ℓ -v diagrams. The fitting of gaussians allows us to obtain the central value, the intensity and the width of the peaks that contributed most in the observed spectra.
Gaussian fits were obtained in the observed HI and CO spectra at each interval of 1 and 2º in longitude for HI and CO (in the galactic plane, i.e. b = 0º, respectively. The results of these procedures are also available since they may also be useful in other studies. Since some points with lower intensities can cause confusion in the identification of the large HI structures, for each spectrum the points were excluded for which the intensity is 30% less than the peak with the maximum intensity. This represents approximately 20% of the points obtained with this fitting procedure.
The ℓ -v diagrams obtained with this gaussian fitting procedure are presented in Figure 4. It can be seen that the HI distribution (Figure 4a) is given almost for the entire Galaxy while the CO emission is mainly predominant in the inner Galaxy (Figure 4b) since the CO is mainly concentrated in the spiral arms (see also Figure 5 of AL05).

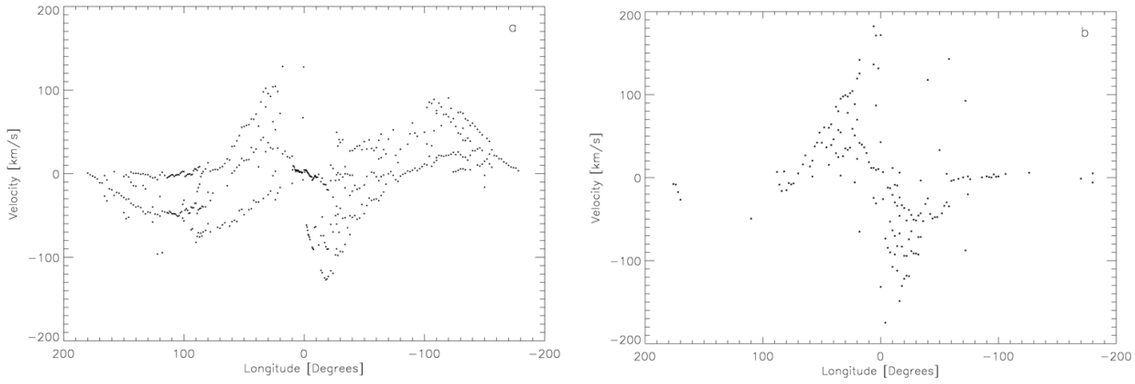

Fig. 4. ℓ -v diagram obtained from the gaussian fits performed for HI (a) and CO (b) spectra

In Figure 4a, one notes the presence of a spiral arm feature for (ℓ,v) = (~ -20,-120º) which also can be seen for HII regions (Amôres 2005). In the case of CO (Figure 4b) it is widely know that this component is distributed in the molecular cloud complexes that constitute the main place for star formation in our Galaxy. The fact that the molecular clouds and the CO emission are good tracers of the spiral structure is related to the interstellar shocks that occur in the spiral arms which produce an increase of the density transforming HI into H_2 (Marinho & Lépine 2000).
In Figure 4b, it is also possible to identify two tangential directions for $\ell \pm 30^o$ and $\ell \pm 50^o$. In the northern Galaxy, the component $\ell \sim 30^o$ splits into two other components, the first one at $\ell \sim 30^o$ and the other at $\ell \sim 25^o$. This feature was first identified by Solomon et al. (1985) from his observations in CO and it is also mentioned by Englmaier (1999). A detailed overview of the main characteristics observed in the ℓ -v diagrams for CO can be found in Fux (1999).

3.3 Description of the empirical models for the spiral arms

From the analysis of external galaxies it can be seen that the spiral logarithm ($\theta \alpha \ln R$) fits real galaxies better than any other spiral curves. In my models the spiral arms are represented by the logarithmic spiral:

$$R = r_0 \exp[(\theta - \theta_0) \operatorname{tg}(i)] \quad (1)$$

in which r_0 and are the polar coordinates which represent the initial arm radius and i is the pitch angle. In this way, to describe a spiral arm four parameters are necessary that specify the arm position in the galactic plane: r_0, θ_0, i, $\Delta\theta$ (the arm length). In addition to these variables, an extra term (δi) was added to the pitch angle in order to produce an effect of variable inclination angle.

Russell & Roberts (1992) from the morphological analysis of the galaxies NGC 5457 and NGC 1232 found an expression to describe the variation of the pitch angle in the spiral arm. This expression is given by $i = \sum A_n (r / r_o)^n$ in which A_n are the coefficients that represent the perturbation term $A_0 \ldots A_3$ e r_0 corresponds to the initial radius of the spiral arm.

A comparison between the observed ℓ-v diagrams and ones obtained from fitting the parameters of the spiral arms will be presented in the next section. The main procedure consists of tracing a sequence of points in the galactic plane, i.e., in the X-Y coordinates (Figure 5a) in order to draw a hypothetical spiral arm segment. The next step consists of verifying whether this represents an observed structure (Figure 5b). If so, it is determined the distance to the galactic center for each point of this arm segment. Once the distance is obtained and its galactocentric radius.

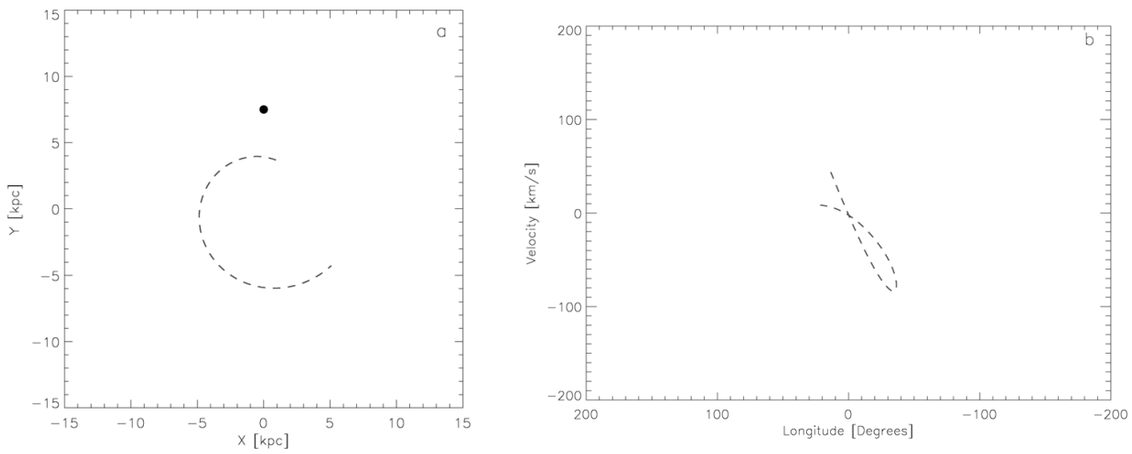

Fig. 5. a-) Arm segment represented in the galactic plane; b-) representation of the same arm in the ℓ-v diagram (the transformation from velocity into position is performed using the Clemens rotation curve and geometric properties).

With the rotation curve, it is possible to plot the longitude and velocity for this point. In short, X-Y positions were transformed into velocities. One position in the X-Y plane gives an unique point in the ℓ-v diagram without distance ambiguity.

Lépine et al. (2001) also presented a similar method to perform the representation of the ℓ-v diagram for HII regions. The main differences between that work and the present one are: i-) I reproduce the ℓ-v diagrams following an empirical scheme which describes the observed characteristics in these diagrams and not for a purely theoretical model; ii-) introduction of the velocity perturbation; iii-) presentation of the tangential directions obtained with my model; iv-) presence of arms with several positions with different pitch angle and; v-) I have used Russeil's catalog instead the Kuchar & Clark (1997) catalog for the HII regions.

In the present work, I also have used a modified Clemens rotation curve which is presented in Figure 6 in which the points represent the original data obtained by Clemens (1985) from

CO data for the interstellar medium. I introduced a modification in the original curve provided by Clemens in order to set R_0 = 7.5 kpc and to use a double exponential as presented below:

$$v_{rot} = 340\exp[-r/20.0 - 1.5/r] + 830\exp[-r/0.73 - 0.3/r] \quad (2)$$

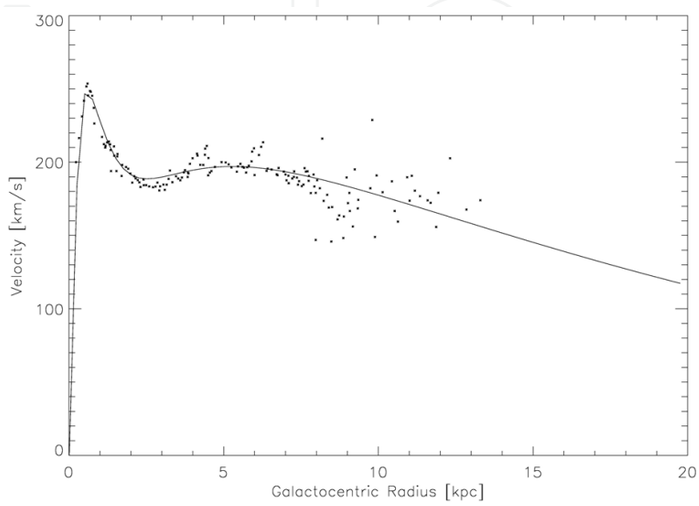

Fig. 6. Rotation curve for our Galaxy determined from the interstellar gas data (Clemens 1985). The lines represent the fit described by the expression above and the points correspond to the data obtained by Clemens.

A similar Clemens rotation curve represented as a double exponential was already presented by Lépine et al. (2001). However, in the present work, I performed a small modification in its parameters in order to improve the quality of the fit. In the present rotation curve, the *rms* errors from the comparison of the observed data and fitted expression by the first expression is equal to 5.043.

So, through the variation of parameters for the spiral arms (expression 1) were determined the best fit for the observed structures in the ℓ-v diagram which is also done verifying whether the face-on representation of the Galaxy is plausible as well whether the tangential directions are in agreement with the observed ones. It is also provide the Xi² total estimate calculated by the expression below:

$$\chi^2 = \frac{1}{N}\sum \min(\sqrt{(l_o - l_c)^2 + (v_o - v_c)^2}) \quad (3)$$

in which N denotes the number of fitted structures, l_0 and l_c are the observed and predicted longitude, with the same notation applying for the velocities v_0 and v_c. The function *min* represents the fact that we get only the point with the least difference. A similar formula was also used by Russeil (2003) in order to estimate the errors involved in the comparisons with her models of spiral arms with the observed HII regions.

Since a simple model of circular velocity does not adequately reproduce some of the characteristics observed in the ℓ-v diagrams, it is also necessary to introduce perturbation terms in the calculated velocities. The use and the justification of these terms were first

described by Ogorodnikov (1958) and is explained in detail by Mishurov & Zenina (1999a.b) and Lépine et al. (2001).

3.3.1 Calculating the perturbed velocities

As explained above, the procedure consists of transforming X-Y galactocentric coordinates of the arms into velocities. So each point with an X-Y coordinate has a corresponding point (ℓ,v) in the ℓ-v diagram that is calculated as explained below. The longitude is directly obtained from X-Y galactic coordinates:

$$\ell = a\tan(\frac{X}{R_0 - Y}) \tag{4}$$

in which R_0 is equal to 7.5 kpc which corresponds to the distance from the Sun to the galactic center. This value is actually largely used and one of the first mentions of its use was by Reid (1993). The final velocity is given by:

$$v = v_1 + v_{\tan y}\cos(\ell) + v_{\tan x}\sin(l) - v_{sun} \tag{5}$$

in which v_{tanx} and v_{tany} are tangential velocities projected in the X-Y plane; and v_1 is calculated from the expression below:

$$v_1 = (V_r(R) + p_{rot})\sin(\ell - \theta) - p_{rad}\cos(\ell - \theta) \tag{6}$$

$V_R(R)$ means the value of the rotation curve for a given galactocentric radius (R), the p_{rot} term corresponds to the perturbation in rotation and v_{sun} is the projected velocity of the Sun calculated by the relation:

$$v_{sun} = V_r(R_0)\sin(\ell) - v_{out}\cos(\ell) \tag{7}$$

in which v_{out} = 12.8 km/s.
The term which describes the radial and angular perturbation components is given by:

$$p_{rad} = a_2\sin(0.2 + a_1 R - 2\theta) \tag{8}$$

The term a_2 is described below:

$$a_2 = -8.0a\log(\frac{R}{r_c}) \tag{9}$$

in which r_c was set equal to 8.3 kpc and represents the co-rotation radius (section 3.5). The term a_1 = -0.4 represents the phase variation. The amplitude of the perturbation in the rotation is described by the expression:

$$p_{rot} = a_3\sin(\phi - 2\theta) \tag{10}$$

in which $a_3 = 12.5*\text{alog}(R/r_c)$. Due to the existence of the LindBlad internal resonance (ILR, see Amaral & Lépine (1997, AL97)), the terms a_2 and a_3 are set equal to zero for r <2.5 kpc. The final values of these constants were obtained after some tests in order to reproduce the characteristics observed in the ℓ-v diagrams for both HI and HII regions.

3.4 Fitting the spiral arm parameters

In the next sub-section, the results of fitting the observed ℓ-v diagrams for the HI will be presented. For each one, it is presented the estimate (Table 2) of the Xi^2 obtained with models in comparison with the observed features as well as the same estimate with the ones obtained with a model of four arms and the superposition of 2+4 spiral arms. In order to reproduce these diagrams, I have manipulated the parameters r_0, θ_0, i, $\Delta\theta$ of the spiral arms described in expression 1.

It should be noted that in performing these fitting procedures the objective is not only to reproduce the observed ℓ-v diagram but also to ensure that the parameters obtained adequately reproduce the Galaxy face-on aspect and the observed tangential directions. In the case of the HI, they should also account for the tangential directions in the longitudinal profile for the integrated intensity (Figure 9).

Figure 7 presents the comparison between the observed ℓ-v and the one obtained after fitting the spiral arms parameters with the respective Galaxy face-on representation provided in Figure 8. In order to better visualize the results, the arms are represented by straight or dashed lines with different colors. The parameters are given in the Table 3. The final Xi^2 for this adjustment calculated by expression 3 is presented in Table 2, which also shows the Xi^2 expected with models of four and the superposition of 2 + 4 spiral arms.

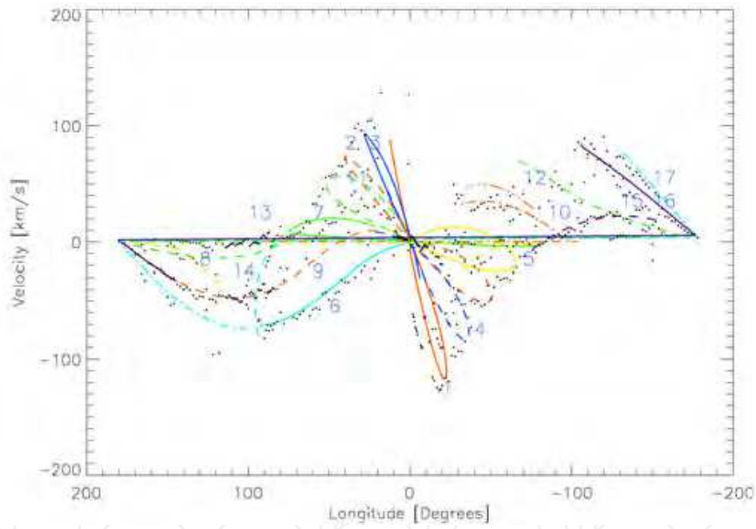

Fig. 7. ℓ-v diagram for the HI. The lines represent the spiral arms and the points the data obtained from the Gaussian fits for HI (section 3.2). The numbers correspond to the arm parameters described in the Table 3.

For the model of 2 + 4 spiral arms I have used the Model proposed by Lépine et al. (2001) with pitch angles equal to 6.8° and 13.5° for the pattern of 2 and 4, respectively. In the case of four spiral arms, the model proposed by Ortiz & Lépine (1993) was used which consists of a model with four spiral arms, all of which begin at r_0 equal to 2.3 kpc and with pitch angle equal to 13.8°, each one separated by a phase of 90°. I also add a local arm with i equal to 12.5° and size equal to 51°.

A number is presented next to each structure (according to the numbers presented in the Table 3). In total, there are 17 structures, among them: arms, bifurcations, bridges. The largest structures correspond to arms 1,2,3,4,7,11, located in the inner Galaxy with initial radius varying from 2.5 to 4.0 kpc.

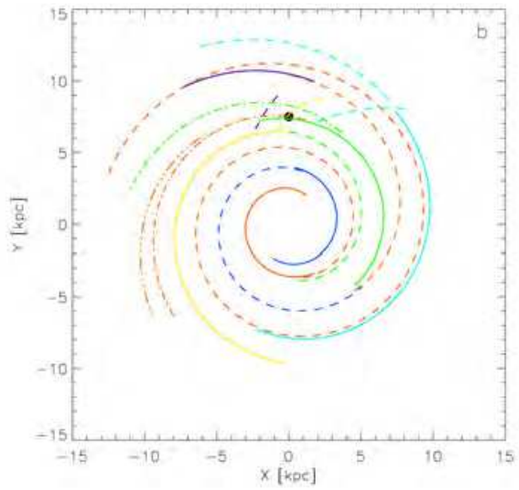

Fig. 8. Face-on Galaxy representation, where the lines represent the spiral arms, with the same colors as Figure 7.

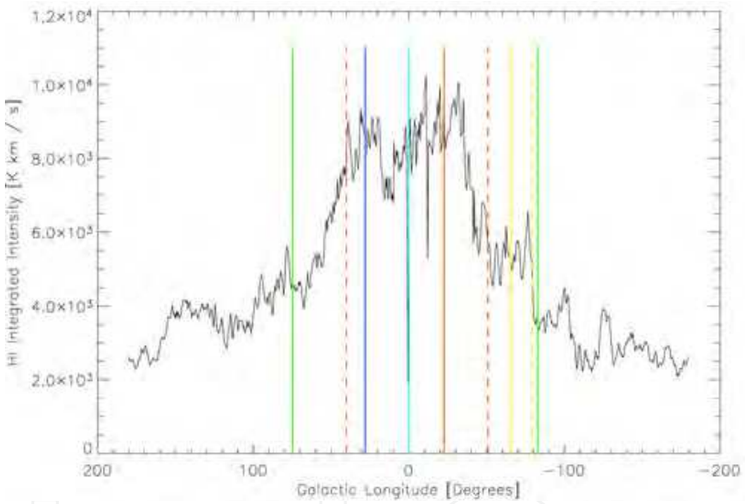

Fig. 9. Longitudinal profile for the integrated intensity for the HI where the vertical lines are the tangential directions predicted by the model.

HI model	5.265
4 arms	17.536
2+4 arms	8.189

Table 2. Comparison between the Xi^2 square estimate obtained from my model and the ones obtained from other models.

Figure 9 shows the longitudinal profile for the integrated intensity for the HI ($b = 0^o$) that was calculated from the HI surveys mentioned in section 3.1. The lines represent the tangential direction for each arm in which the color follows the same representation adopted above. Below a brief discussion is provided about each structure. Arm 7 with $r_i = 6.22$ kpc is one exception of a long arm that does not begins at low radius. Arm 5, which is represented

by the thin yellow line which can be seen in Figure 7, is a prolongation of arm 11 (green dashed). Arm 11 has r_i = 3.95 kpc with pitch angle equal to 9.40°.
However, to continue describing this arm and reproduce adequately the observed ℓ-v diagram it is necessary to introduce a new arm structure with the pitch angle slightly changed. This is done changing mainly the parameters θ and r_i in order to coincide with the arm end. Note that without this modification the loop extremity will fall in (~ -70,-10°) and not in (~-65,-20°) which represents a better description for the structures observed for the HI in this direction. In summary, structures 5 and 11 represent a unique arm with a modified pitch angle in order to reproduce the observed ℓ-v diagram. It should be noted that arms with variable pitch that can also can be seen in other galaxies, such as M 81, for example.

arm	i (°)	radius (kpc)	initial phase (°)	δi (°)	size (°)
1	6.60	2.35	-31.0	0.0	240
2	6.70	3.80	195.0	0.0	330
3	7.10	2.57	155.0	0.0	200
4	7.50	3.80	-14.0	0.0	245
5	6.35	7.50	-2.50	0.0	182
6	7.50	7.60	163.0	0.0	155
7	4.20	6.22	228.0	0.0	149
8	-20.30	9.02	345.0	-1.80	24
9	11.55	6.44	225.0	0.0	135
10	7.77	7.36	-8.40	0.05	139
11	9.40	3.95	190.0	0.0	170
12	11.50	8.60	45.40	0.00	79
13	12.80	7.35	330.0	0.00	109
14	-40.0	11.40	315.0	0.0	31
15	12.0	10.10	-10.0	0.0	48
16	9.00	5.00	-45.0	0.1	25
17	11.10	11.10	-38.0	0.0	65

Table 3. Main parameters for the arms used to fit the ℓ-v diagram for the HI. Each number represents the arm in the figure 7.

A similar characteristic is noted for arms 2 (dashed red), 6 (light blue) and 17 (dashed blue light). In this case, if we increase the size of arm 2 (Figure 10a e 10b) without changing the i and r_i we obtain an inadequate description of the HI distribution at $0° < \ell < -100°$. Arm 6 is a prolongation of arm 2, but with i = 7.5, which better represents the HI distribution in this region with the line that passes through arm 6 (light blue) providing a good match for almost all of the points in this direction. Arm 17 matches better the structures observed in $-140° < \ell < -170°$ than arm 2. The i of the arm 17 is equal to 11.1°. An interesting characteristic can be seen at the end of this structure which corresponds to a bifurcation (arm 14) as well as the beginning of the other spiral arm (arm 17).
In the Galaxy face-on representation one also notes three structures that resembles bridges (arms 8,10,14), two of them with $i < 0$. These structures were introduced in order to reproduce the observed ℓ-v diagram. Structure 14 matches most of the points from $\ell \sim -70°$ to $\ell \sim -150°$. These structures could be explained by the proximity of the Sun to the co-rotation point (see section 5). Similar characteristics were also assumed by De Simone et al. (2004).

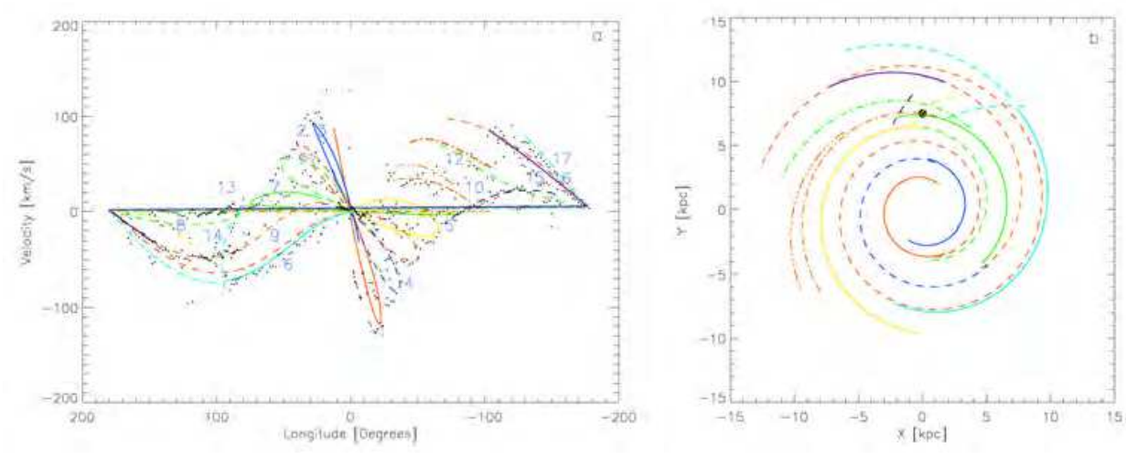

Fig. 10. a-) ℓ -v diagram with the modification of the extension for the arm 2 (red dashed) from 330 to 600º; b-) face-on aspect for this set of arm parameters. The color and the representation are the same adopted in figures 7, 8 and 9.

The violet dashed line (arm 14) in Figure 8 represents a structure that seems to be a bifurcation that begins in arm 15 (heavy green line). This arm describes the structures around ℓ < -100º in ℓ -v the diagram. Based on Figure 7, we observe that arm 9 reproduces adequately the structures observed in the ℓ -v diagram for ℓ > 80º. This arm is a prolongation of arm 4 with i = 11.55. The continuation of arm 9 is arm 16 (heavy blue line) with i = 9.0.
McClure-Griffiths et al. (2004), while analyzing ATCA data, detected a structure that extends from ℓ = 260º to 330º that they attributed to a spiral arm with i = 9.0º. This structure was also found in our results as represented by arm 12 with i = 11.5º. Kerr (1969) published latitude-velocity diagrams in which a bridge appears in the third quadrant toward positive velocities. Kerr (1969) also presented maps with this feature extending from ℓ = -150º to -70º. Davies (1972) also interpreted this region as relating to the end of a spiral arm associated with high velocity clouds.

3.5 Co-rotation radius

Since the first HI observations the existence of a hole was seen in its distribution in the Galaxy (Kerr 1969 and Burton & Gordon 1978). In these works, the authors noted a gas deficiency in the radial gas distribution for R = 11 kpc, assuming R_0 = 10 kpc. From the theoretical point of view Marochnik et al. (1972), Crézé & Mennessier (1973) and AL97 also found evidence that the co-rotation point, i.e., the point where the rotation velocity of the spiral pattern coincides with the rotation curve of the gas and stars could be located in the Solar neighborhood. The effect of the co-rotation can be understood in the following terms: there is a region where movement exists pumping the gas inside and outside resulting in a deficiency of the gas in these regions. This effect was also studied in detail by Suchkov (1978), Goldreich & Tremaine (1978), Gorkavyi & Fridman (1994). Mishurov & Zenina (1999a) also found evidence that the co-rotation point would be located near the solar radius.
Amôres, Lépine & Mishurov (2009, ALM09) analyzed the HI spectra of the whole galactic longitudes range in steps of 0.5º, with galactic latitudes in steps of one degree in the range ± 5º, plus the additional latitudes ± 10º detecting for each spectrum the velocity of the deep

minima which are present, simply by identifying the channel with the lowest value of antenna temperature.
They obtained that distribution of the density minima in the galactic plane, derived from their kinematic distances from the Sun (is shown in Figure 11). The minima observed at different latitudes are all projected on the galactic plane. The ring-shaped gap is circular and very clear. It looks like the Cassini division in Saturn's rings.

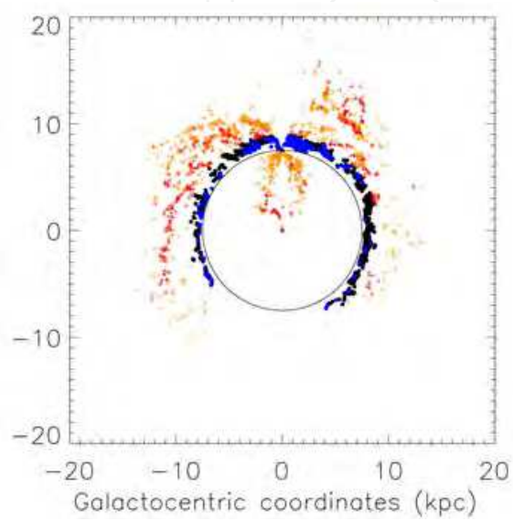

Fig. 11. Galactocentric distance distribution of the gaps for the whole sample of measurements including different latitudes. The Gaussian fit is centered at 8.25 kpc (Adapted from ALM09, figure 4).

The analysis of HI spectra allows to determine the points in which the HI has a gap in its distribution by means of an empirical method. The histogram with the galactocentric radius of each one of these gaps showed that the most of them are located nearest the solar radius which highlights the fact that the Sun is located at the co-rotation point in the Galaxy.

4. Interstellar extinction

One of the main difficulties in the study of both properties of individual objects and the galactic structure resides in the interstellar extinction determination. However, due to the clumpiness distribution of the interstellar dust, it is difficult to model it. Several works have been done in order to model the interstellar extinction distribution in the Galaxy, as presented by Arenou et al. (1992), Hakkila et al. (1997), Méndez & van Altena (1997), Drimmel et al. (2003), Amôres & Lépine (2005), Marshall et al. (2006) among others. In addition, some maps were elaborated in order to provide the integrated extinction along the line of sight, as the Burstein & Heiles (1978,1982), Schlegel et al. (1998, SFD) for the whole Galaxy, Schultheis et al. (1998) and Dutra et al. (2003) for the galactic center region, as well as Dobashi et al. (2005) map for A_V for the whole Galaxy ($|b| < 40^o$) based on the star counts method.
It is very important and fundamental for many studies to know the interstellar distribution in our Galaxy. This could be useful for estimation of distances and color corrections of

objects for which the distance can be obtained by some other method, for star counts and brightness models of the Galaxy, also for spectrum extinction correction, among other applications. In this context, we are developing a VO-Service called GALExtin (http://www.galextin.org) that provides the interstellar extinction estimate for any direction in the sky from: 2D maps and 3D models available and catalogs with extinction measure as well as diffuse emission. It is also useful to study the distribution of interstellar extinction towards star clusters. This service is very useful since most of the models and maps require the installation of programs and large files. The users may provide a list with coordinates and distances and the GALExtin (Amôres et al. 2011a) will produce as an output a list with extinction estimates for each object for a chosen model.

The determination of the interstellar extinction is fundamental for all fields of astronomy, from stellar studies in which it is important to know the extinction towards a given object from its coordinates and distances (3D Models), to extragalactic astronomy field; in this case it is mandatory to know the contribution of the extinction of our Galaxy along the line of sight.

Amôres & Lépine (2005) proposed two models to describe the interstellar extinction in the Galaxy (http://www.astro.iag.usp.br/~amores) both based on the hypothesis that gas and dust are homogeneously mixed, and that consequently, the known distribution of the gas can be used to describe the dust distribution. In the first model (model A) it was assumed that the Galaxy presents azimuthal symmetry, with the gas density depending only on the Galactic radius and on the distance from the galactic plane; as a result, in any direction the extinction increases smoothly with the distance from the Sun. In the second model (model S) the spiral structure of the Galaxy was taken into account; the parameters of the spiral arms were adjusted by fitting the observed longitude-velocity diagrams of different tracers, such as: CO, 100 μm, HI and H II regions (Amôres, 2005). In this model the integrated extinction grows by steps each time a spiral arm is crossed, and remains almost constant in the inter-arms regions (Amôres & Lépine 2007, AL07).

In this latter work, AL07 compared the extinction models with a sample of globular and open cluster and elliptical galaxies. From the comparison with elliptical galaxies the difference between Model A and Burstein & Heiles (1978) and Schlegel et al. (1998) were around 20-30 %. Figure 12 shows a map with the comparison with SFD maps for whole sky with δ E(B-V), i.e. difference between Model A and the SFD maps.

As pointed by AL07 it can be seen regions (indicated by white color) in which the Model A2 predicts less extinction than provided by SFD, i.e., the $\delta E(B-V) < -0.4$, notably around $150^o \leq \ell \leq 200^o$, in a region that extends towards negative latitudes. This region was also pointed by B03 as the region where there is a high variation in the gas-to-dust ratio.

The resolution and coverage of the different models and maps is another point that should be taken into account in the extinction studies. There are models that provide better estimates in the solar neighborhood up to distances equal to 1.0 kpc, while they fail to describe extinction outside this distance. On the other hand, there are models that provide better values at 3.0 kpc, but being imprecise at low distances. Depending on the assumptions used in their elaboration, some models can be used only for a given region in the sky.

Another interesting issue in galactic extinction is the combination of different models. In this sense, Amôres & Robin (2011) studied the variation for interstellar extinction along a line of sight joining the results from AL05 and Marshall et al. (2006, M06).

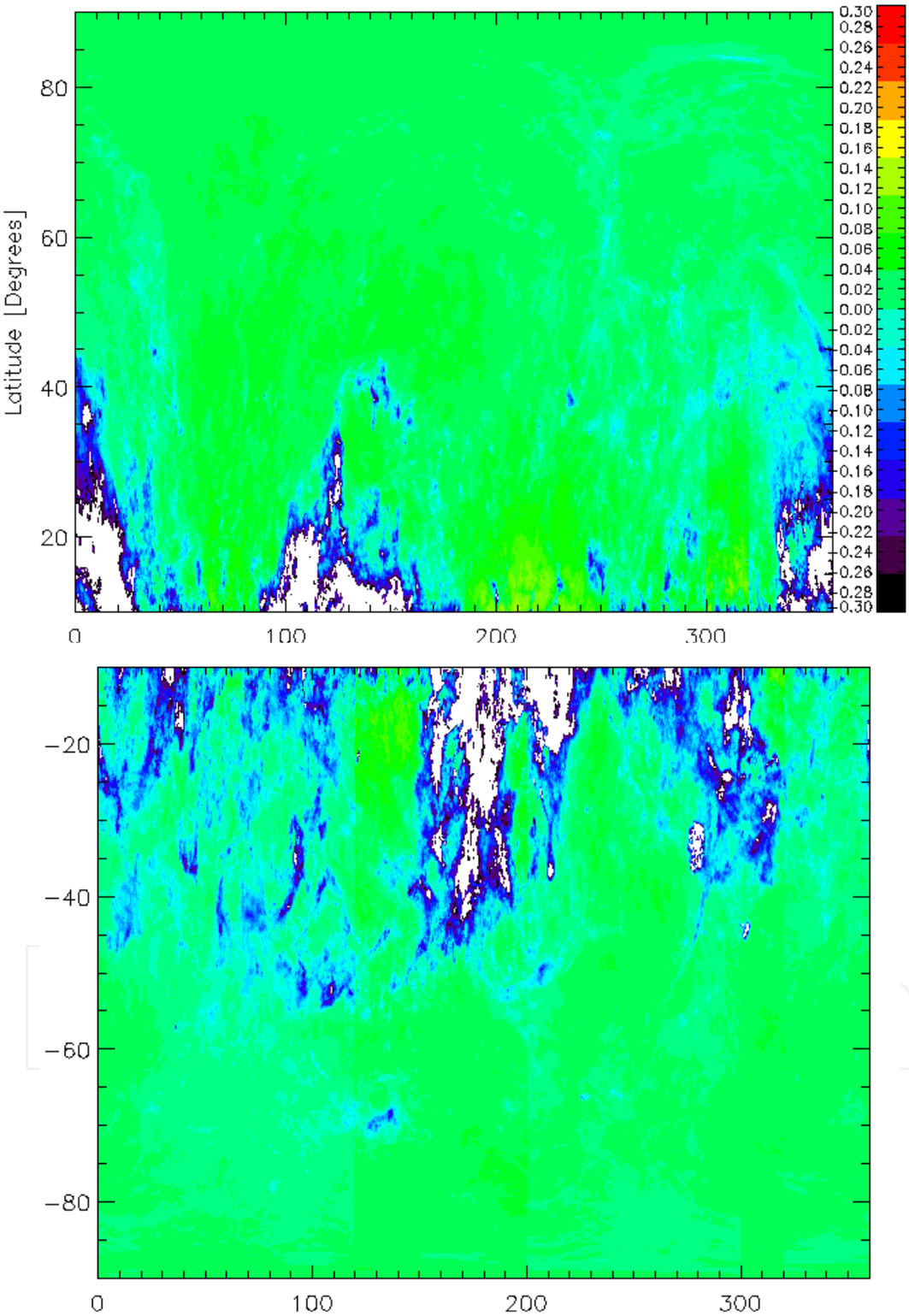

Fig. 12. Map in galactic coordinates of $\delta E(B - V)$ from the comparison of AL07 model with SFD98 for the whole Galaxy, using a grip spacing of 0.25° in l and b (Adapted from AL07, figure 3).

5. Star counts simulations

Star counts models have been largely used in astrophysics. They constitute an important and useful tool to study the galactic structure and its evolution. In particular, the Besançon Galaxy Model (BGM) provides a Galaxy description in the evolutive point of view joining both the kinematics and dynamics properties. One of the main differences in relation to others star counts models resides in the fact that the BGM is dynamically self-consistent (Bienayme et al. 1987).

The Besançon Galaxy Model (BGM) has been employed in a series of astrophysical applications (Robin et al. 2003). In the context of the GAIA mission, the BGM is the Model used to simulate the stellar content of our Galaxy. Amôres et al. (2007) presented a comparison and the improvements performed in the BGM - Java version in order to produce similar results as produced by the BGM in the Fortran version. Robin et al. (2009) also presented expected observations that will be performed by GAIA using BGM.

Amôres & Robin (2011) are using BGM in order to retrieve the parameters of spiral arms and other Galactic parameters, as warp flare by comparing BGM results with 2 MASS observations using the genetic algorithms.

On the other hand, Amôres et al. (2010) also presented simulations for the expected observations that will be performed by VVV. Vista Variables In The Via Láctea (VVV) is an ESO variability (Minniti, D., et al. 2010) survey that is performing observations in near infrared bands (Z,Y, J,H and Ks) towards the galactic bulge and part of the disk, totalizing an area of 520 square degrees. A total of 1920 observation hours (2009-2013) will be used at VISTA, within a 5 year time lapse.

In order to predict star counts distribution towards the VVV region we made use of TRI-Legal Galaxy Model (Girardi et al. 2005, G05) with galactic parameters as pointed by Vanhollebeke et al. (2009) and G05 considering VVV completeness limit, i.e. K = 20.0. For other filters, we have cut (after simulation) at other VVV limits, i.e. Z= 21.6, Y = 20.9, J = 20.6, H =19.0. The results are presented by Amôres et al. 2011b.

Since VVV observes galactic plane regions it is very important to know the interstellar extinction (Amôres et al. 2009) distribution towards them. We made use of 3D Marshall et al. (2006) interstellar extinction model. TRI-Legal predicts the star counts taking into account three galactic components, i.e. bulge, disk and halo. For each simulated star there is a set of properties as its distance, magnitude, gravity, temperature among others. From temperature we determine the spectral type.

6. Conclusions

Concerning HI model to describe spiral arms positions from HI data, the results presented in this chapter allow us to obtain the spiral arm positions based on HI distribution obtaining the spiral arm parameters (r_0, θ_0, i, $\Delta\theta$) which reproduce the main observed features in the ℓ -v diagrams for HI. The tangential directions predicted by models are also consistent with the ones predicted by other models, such as for instance the one proposed by Englmaier (1999, see his Table 1), as can be seen in the peaks existent in the longitudinal profiles for HI (Figure 9).

It should be noted that it is not being proposed a Galaxy with too many spiral arms, 17 for the atomic hydrogen since many of the structures presented in this chapter only represent prolongations of arms with different pitch angles which was necessary in order to adequately reproduce the observed ℓ -v diagram.

This is because a more simplified model would not be realistic. Many arm segments with different pitch angles are needed because real arms are not well represented by a single logarithmic spiral that follows a long path around the Galaxy. Furthermore, there are bifurcations and some short bridges. Another difficulty related to HI consists in the fact that these components are not only predominantly concentrated in the spiral arms, such as the CO, for example. Instead, there is also an amount of HI in the inter-arm regions.
In this sense, the use of the method proposed by Amôres & Lépine (2004) will also allow to reproduce not only the positions of the arms but also their density, allowing the elaboration of numerical ℓ-v diagrams, to estimate width of the arms since they are not as thin and well-resolved as presented here.
In relation to interstellar extinction important results are also being obtained from the inter-comparisons of different values of interstellar extinction obtained from Planetary Nebulae (PNe). Köppen & Amôres (2011) have used a large sample of PNe towards the galactic disk and bulge in order to obtain average values for interstellar extinction as well as to review the old values, most of the times obtained with different extinction curves.
A good estimate of interstellar extinction is also important in the study of Supernovae. Arsenijevic & Amôres (2011) have compared the distribution of interstellar extinction towards supernovae and also presented a new method to reproduce observed spectra using the Genetic Algorithms and basic parameters as galactic and galaxy host extinction and R_V (the ratio of the total to selective extinction). The use of global optimization methods can be a powerfull tool to obtain parameters from large surveys.

7. Acknowledgements

E. B. de Amôres acknowledges support from FCT under grant no. SFRH/BPD/42239/2007 and also Laboratory for Systems, Instrumentation and Modeling in Science and Technology for Space and the Environment (SIM), funded by "Fundação para a Ciência e a Tecnologia" thought Portuguese National Funds.

8. References

Adelman-McCarthy, J. K.; et al., 2009, VizieR On-line Data Catalog: II/294
Amaral, L. H. & Lépine, J. R. D. 1997, MNRAS 286, 885 (AL97)
Amôres & Lépine, 2004, Milky Way Surveys: The Structure and Evolution of our Galaxy, Proceedings of ASP Conference 317. Edited by Dan Clemens, Ronak Shah, and Teresa Brainerd. San Francisco: Astronomical Society of the Pacific, 2004, 317
Amôres , E. B., 2005, PhD Thesis, Universidade de São Paulo
Amôres, E. B. Lépine, J. R. D. 2005, AJ, 130, 679 (AL05, Paper I)
Amôres, E. B. Lépine, J. R. D. 2007, AJ, 133, 1519
Amôres, E. B. Lépine, J. R. D. 2009, Mishurov, Y., MNRAS, 400, 1768
Amôres, E. B. ; Moitinho, A. ; Arsenijevic, V, Sodré Jr., 2011, GALExtin: A VO-Service to estimate galactic interstellar extinction. In: Jenam 2011 Stars clusters in the Era of Large Scale-Surveys, 2011 Lisboa. Proceedings of Stars clusters in the Era of Large Scale-Surveys, 2011
Amôres, E. B. ; Padilla, N. ; Sodré Jr., L. ; Minniti, D. ; Barbuy, B., 2011, Simulations of star and galaxies counts towards Vista Variables in the Via Láctea survey region. In:

Environment and the formation of galaxies: 30 years later, 2011, Lisboa. Proceedings of Environment and the formation of galaxies: 30 years later, 2011.
Amôres, E. B., Robin, A. C., 2011, in preparation
Amôres, E. B., Robin, A. C., Luri, X., Masana, E., Reylé, C., Babusiaux, C. , 2007Use of the Besançon Galaxy Model for the Gaia Mission Simulator. In: VII Scientific Meeting of the Spanish Astronomical Society (SEA), Barcelona. Highlights of Spanish Astrophysics IV. Proceedings of the VII Scientific Meeting of the Spanish Astronomical Society (SEA). Dordrecht : Springer-Verlag, 2007
Amôres, E. B., Sodré, Jr., L, Barbuy, B., 2009, Low extinction windows in the VVV survey region. In: Special Session 8 at the IAU General Assembly 2009 - The Galactic Plane, in depth and across the spectrum, 2009, Rio de Janeiro. Highlights Of Astronomy, 2009. V. 15.
Arenou, F., Grenon, M. & Gomez, A. 1992, A&A, 258, 104
Arsenijevic, V., Amôres, E. B., 2011, submitted to MNRAS
Bajaja, E., Arnal, E. M., Larrarte, J. J., Morras, R., Pöppel, W. G. L., Kalberla, P. M. W., 2005, A&A, 440, 767
Bienaymé, O., Robin, A.C., Crézé, , M. 1987, A&A, 180, 94
Burstein D., Heiles, C. 1978, ApJ 225, 40
Burstein D., Heiles, C. 1982, AJ 210, 341
Burton, W. B., Gordon, M. A., 1978, A&A, 63, 7
Burton, W. B., & Liszt, H. S. 1983, A&AS, 52, 63
Burton, W. B., Liszt, H. S.,1993, A&A, 274, 765
Clemens, D. P., Sanders, 1985 ApJ 295, 422
Clemens, D. P.; Sanders, D. B.; Scoville, N. Z.; Solomon, P. M., 1986, ApJ Suppl. Series, 60, 297
Crézé, M., 1973, Mennessier, M. O., A&A, 27, 281
Cutri, R. M, et al., 2003, VizieR On-line Data Catalog: II/246
Dame, T. M., Ungerechts, H., Cohen, R. S., de Geus, E. J., Grenier, I. A., May, J., Murphy, D. C., Nyman, L.-A., Thaddeus, P., 1987,ApJ, 322, 706
Dame, T. M., Ungerechts, T. M., Cohen, R. S., Thaddeus, P., 2001, ApJ, 547, 792
Davies, R. D., 1972, MNRAS, 160, 381
De Simone, R., Wu, X., Tremaine, S., 2004, MNRAS, 350, 627-643
DIRBE Explanatory Supplement, 1998, http://lambda.gsfc.nasa.gov/product/cobe/dirbe_exsup.cfm
Dobashi, K. et al. 2005, PASJ, 57, 1
Drimmel, R., Cabrera-Lavers, A. & López-Corredoira, M. 2003, A&A, 409, 205
Dutra, C. M.; Santiago, B. X.; Bica, E. L. D.; Barbuy, B., 2003, MNRAS, 338, 253
Englmaeir, P. & Gerhard, O. 1999, MNRAS 304,512
Fux, R., 1999, A&A, 345, 787
Girardi,L.; Groenewegen,M.A.T., Hatziminaoglou,E., da Costa,L., 2005, A&A, 436, 895
Goldreich, P., Tremaine, S., 1978, Icarues, 34, 227
Gorkavyi, N. N., Fridman, A. M., 1994, Physics of Planetary Rings: Celestial Mechanics of Continiuous Medium, Moscow : Nauka
Hakkila, J. et al. 1997, AJ, 114, 2043
Hartmann D., Burton W.B., 1997, Atlas of Galactic Neutral Hydrogen, Cambridge University Press

Haud, U., Kalberla, P. M. W., 2007, A&A, 466, 555
Hauser, M., et al. 1984, ApJ, 285, 74
Jarrett, T. H., Chester, T., Cutri, R., Schneider, S., Skrutskie, M., Huchra, J. P., AJ, 2000, AJ, 119, 2498
Kalberla P.M.W., Burton W.B., Hartmann D., Arnal E.M., Bajaja E., Morras R., Poeppel W.G.L., 2005, A&A, 440, 775
Kalberla, P. M. W., Haud, U., 2006, A&A, 455, 481
Kerr, F. J., 1969, ARA&A 7, 163
Kerr, F. J., Bowers, P. F., Jackson, P. D., Kerr, M., 1986, A&A Suppl. Series, 66, 373
Köppen, J., Amôres, E. B., 2011, in preparation
Kuchar, T. A, Clark, F. O., 1997, ApJ, 488, 224
Lépine, J. R. D., Mishurov ,Y. & Dedikov, Y. 2001, ApJ, 546, 234
Majewski, Steven R.; Skrutskie, M. F.; Weinberg, Martin D.; Ostheimer, James C., 2003, ApJ, 599, 1082
Marinho, E. P., Lépine, J. R. D., 2000, A&A, 142, 165
Marochnik, L. S., Mishurov, Yu. N., Suchkov, A. A., 1972, Ap&SS, 19, 285
Marshall, D.J., Robin, A.C., Reyl\'{e}, C., Schultheis, M., Picaud, S., 2006, A&A, 453, 635
Mendez, R. A. & van Altena, W. F. 1998, A&A, 330, 910
McClure-Griffiths, N. M., Dickey, J. M., Gaensler, B. M., Green, A. J., 2004, ApJ, L127
Minniti. D., et al., 2010, New Astronomy, V. 15, Issue 5, p. 433-443
Mishurov ,Yu., Zenina, I. A., 1999a, A&A, 341, 81
Mishurov, Yu., Zenina, I. A., 1999b, Astronomy Reports, 43, 487
Ogorodnikov, K.F. 1958, The Stellar System Dynamics, Physical-Mathematical Publishing House, Moscow, USSR
Ortiz, R., Lépine, J. R. D., 1993, A&A, 279, 90
Paladini, R., Davies, R. D., DeZotti, G., 2004, MNRAS, 347, 237
Reid, M. J., 1993, ARA&A, 31, 345
Robin,A. C.,Reylé, C.,Derriere, S.,Picaud, S. 2003, A&A, 409, 523
Robin, A. C.; Reylé, C.; Grux, E.; The Gaia Dpac Consortium, 2009, SF2A-2009: Proceedings of the Annual meeting of the French Society of Astronomy and Astrophysics, held 29 June - 4 July 2009 in Besançon, France. Eds.: M. Heydari-Malayeri, C. Reylé and R. Samadi, p.79
Russeil, D. 2003 A&A, 397, 133
Russell, W. S., Roberts, W. W., 1992, ApJ, 398, 94
Skrutskie, M. F. et al., 2006, AJ, 131,1163
Schlegel, David J., Finkbeiner, Douglas P., Davis, Marc,1998, ApJ, 500, 525
Schultheis, M., Ganesh, S., Simon, G., Omont, A, Alard, C., Borsenberger, J., Copet, E., Epchtein, N. Fouqué, P., Habing, H., 1999, A&A, 349, L69
Solomon, P. M., Sanders, D. D., Rivolo, A. R., 1985, ApJ, 292, 19
Suchkov, A. A., 1978, AZh, 55, 972
Vanhollebeke, E, Groenewegen, M. A. T., Girardi,L., 2009, MNRAS, 498, 95
Weaver, H., Williams, D. R. W.: 1973, A&A Suppl. Series, 8, 1
Zacharias et al. 2010, AJ, 139, 2184

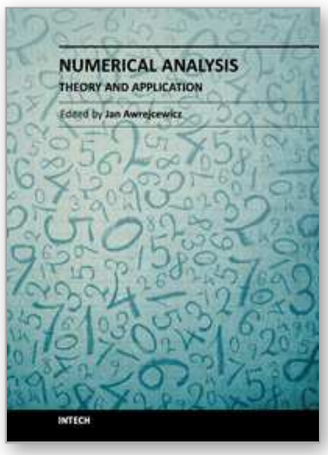

Numerical Analysis - Theory and Application

Edited by Prof. Jan Awrejcewicz

ISBN 978-953-307-389-7
Hard cover, 626 pages
Publisher InTech
Published online 09, September, 2011
Published in print edition September, 2011

Numerical Analysis â€“ Theory and Application is an edited book divided into two parts: Part I devoted to Theory, and Part II dealing with Application. The presented book is focused on introducing theoretical approaches of numerical analysis as well as applications of various numerical methods to either study or solving numerous theoretical and engineering problems. Since a large number of pure theoretical research is proposed as well as a large amount of applications oriented numerical simulation results are given, the book can be useful for both theoretical and applied research aimed on numerical simulations. In addition, in many cases the presented approaches can be applied directly either by theoreticians or engineers.

How to reference

In order to correctly reference this scholarly work, feel free to copy and paste the following:

Eduardo B. de Amôres (2011). Data Analysis and Simulations of the Large Data Sets in the Galactic Astronomy, Numerical Analysis - Theory and Application, Prof. Jan Awrejcewicz (Ed.), ISBN: 978-953-307-389-7, InTech, Available from: http://www.intechopen.com/books/numerical-analysis-theory-and-application/data-analysis-and-simulations-of-the-large-data-sets-in-the-galactic-astronomy

INTECH
open science | open minds

InTech Europe
University Campus STeP Ri
Slavka Krautzeka 83/A
51000 Rijeka, Croatia
Phone: +385 (51) 770 447
Fax: +385 (51) 686 166
www.intechopen.com

InTech China
Unit 405, Office Block, Hotel Equatorial Shanghai
No.65, Yan An Road (West), Shanghai, 200040, China
中国上海市延安西路65号上海国际贵都大饭店办公楼405单元
Phone: +86-21-62489820
Fax: +86-21-62489821

IntechOpen